Advanced Robotics

ISSN: 0169-1864 (Print) 1568-5535 (Online) Journal homepage: http://www.tandfonline.com/loi/tadr20

Statistically optimized FOPID for output force control of SEAs

Somayeh Norouzi Ghazbi, Alireza Akbarzadeh & Iman Kardan

To cite this article: Somayeh Norouzi Ghazbi, Alireza Akbarzadeh & Iman Kardan (2018) Statistically optimized FOPID for output force control of SEAs, Advanced Robotics, 32:5, 231-241, DOI: 10.1080/01691864.2018.1431150

To link to this article: https://doi.org/10.1080/01691864.2018.1431150

Published online: 12 Feb 2018.

ADVANCED ROBOTICS, 2018
VOL. 32, NO. 5, 231–241
https://doi.org/10.1080/01691864.2018.1431150

FULL PAPER

Statistically optimized FOPID for output force control of SEAs

Somayeh Norouzi Ghazbi, Alireza Akbarzadeh and Iman Kardan

Center of Excellence on Soft Computing and Intelligent Information Processing (SCIIP), Mechanical Engineering Department, Ferdowsi University of Mashhad, Mashhad, Iran

ABSTRACT

Fractional order PID (FOPID) controllers have recently found an increasing application in different fields of control. Comparing to traditional PID algorithms, FOPID controllers provide more flexibility and better performances. The simple and non-model-based structure of FOPID controllers has boosted their usage in real-world applications. However, due to having two more control parameters than regular PID controllers and the non-linear structure of FOPID controllers, the tuning procedure of these controllers is still a challenge. The authors of the present paper have recently proposed a Taguchi-based gain tuning algorithm for tuning of control parameters of FOPID controller. The present paper is an experimental evaluation of the proposed method. A custom made SEA, FUM-LSEA, is used as the test bed in this study. Deriving a dynamic model of the FUM-LSEA, feed-forward terms are added to the controller to compensate for disturbances from motions of the output block. Optimal gains and orders of the controller are obtained through a set of experiments suggested by the Taguchi method. The Taguchi optimized controller is also compared to a Ziegler–Nichols tuned controller. The experimental results indicate 45% improvements in force tracking error.

ARTICLE HISTORY
Received 26 January 2017
Revised 30 June 2017
and 29 November 2017
Accepted 25 December 2017

KEYWORDS
SEA; FOPID; Taguchi; tuning; ANOVA

1. Introduction

Series elastic actuators (SEAs) are variable stiffness actuators including an elastic element, e.g. a spring that is placed between the actuator's motor and the load. The elastic element is used to elastically decouple the actuator from the load and to improve tolerance to mechanical shocks. If proper stiffness is selected according to the target task, the spring can also protect the motor in case of unwanted collisions of the output link [1,2]. Advantages of SEAs over stiff actuators are low and adjustable output impedance, low friction, impact resistance, increased efficiency due to energy storage and increased stability. The mentioned advantages, that are well studied by Pratt et al. in Ref. [3], nominate SEAs as suitable choices for human-assistive robotic systems. As shown in Figure 1, a custom prismatic SEA, called FUM-LSEA [4], is used in the present work. This actuator is constructed in the Robotic lab of Ferdowsi university of Mashhad.

As shown in Figure 1, in FUM-LSEA, two separate springs are put around the central ball-screw, acting in parallel to each other and in series to the actuator's motor and the output link. The linear motions of the actuator are produced by a ball-screw mechanism with a lead of 5 mm. A belt and pulley system with a ratio of 2:1 transfers motions from the AC servo motor to the ball-screw and increases the motor torques. A magnetic linear incremental encoder is used to measure the deflections of the springs and measure the output force of the actuator.

One increasingly popular application of SEAs is for human assistive robots that have been intensively developed in recent years [1,5]. Human assistive robots are systems that assist human motions with actuation capabilities. To effectively assist human motions, actuators with capability of generating large torques are required. In human-assistance scenarios, the actuator is connected to single or multiple joints of human in order to provide assistive torques. As there is a connection between the patient and the system, meeting precise control demands is also very important and required. Therefore, precise control of these actuators has drawn lots of attentions in recent years. Control of a SEA with PID-type controller is proposed by Au et al. [4]. Kong et al. [6] has presented force control of a rotary SEA. A study on force control of a SEA with torsion spring using PID controller is reported by Taylor [7] in 2011. Hutter et al. [8] studied fast position control of high compliant SEAs. Misgeld et al. [9] studied robust control of adjustable compliant actuators. In [10], Wang et al. addressed the Sliding Mode control of the SEA using an extended disturbance observer. Adaptive state feedback control of a rotary SEA is also studied in [11].

CONTACT Alireza Akbarzadeh ali_akbarzadeh@um.ac.ir

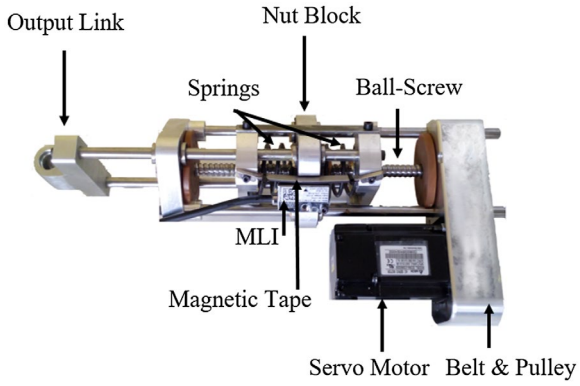

Figure 1. FUM-LSEA used in the present work.

The fractional order calculus constitutes the branch of mathematics that deals with derivatives and integrals from non-integer orders. Recently, fractional order proportional–integral–derivative (FOPID) controllers have received considerable attentions both from academic and industrial points of view. As there are five parameters to adjust instead of three in standard PID type controllers, these controllers provide more flexibility in controller design. However, this also implies that tuning of the controller can be much more complex. During the last years, several techniques have been suggested for tuning the gains and orders of FOPID controllers. The concept of FOPID controller and its better performance in comparison with the classical PID controller was firstly introduced by Podlunbny et al. [12] in 1997. Vinagre et al. [13], studied the FOPID controllers by taking a frequency domain approach. An important step in implementation of PID and FOPID algorithms is to adjust the controller gains and parameters for obtaining a desirable performance. An optimization method is presented by Monje et al. [14] where the parameters of the FOPID are tuned with predefined methods. In 2006, Valerio and Costa [15] proposed Ziegler–Nichols tuning rules for FOPID controllers. An optimization method with particle swarm optimization is reported by Zamani et al [16]. A tuning and auto tuning method for FOPID controllers based on gain crossover frequency and phase margin is proposed by Monje et al. [17].

Taguchi method is a statistical optimization technique, which has the benefit of finding the optimal parameters through significantly reduced number of experiments. Unique features of the Taguchi method nominate it as a powerful practical gain tuning tool. Lee and Kim [18] studied gain tuning for multi-axis PID control systems using the Taguchi method. Ryckebusch et al. [19] used the Taguchi method for tuning PID controller parameters in a multivariable plant. Another Taguchi-based tuning method for two-degrees of freedom proportional–integral controller is reported by Alfaro et al. [20]. Self-tuning mechanism of PID controller based on Taguchi method is reported by Santhakumar and Asoka [21]. Ghazbi and Akbarzadeh [22] compared the performance of the FOPID controllers tuned by particle swarm optimization (PSO), imperialist competitive algorithm (ICA) and genetic algorithm (GA). The simulation results showed the outperformance of the PSO-tuned controller. Ghazbi and Akbarzadeh [23] also proposed the application of Taguchi method for the tuning of FOPID controllers. They applied the Taguchi tuned controller to a simplified dynamic model of the FUM-LSEA and compared the simulation results with those obtained from Ziegler–Nichols. The Taguchi-tuned controller is also compared with a PID controller tuned by genetic algorithm (GA). The results verify the effectiveness of the Taguchi method in tuning of FOPID controllers. However, to the best of the knowledge of the authors, there is no published work on experimental application of the Taguchi method in optimization of FOPID parameters.

This paper proposes an experimental evaluation of the Taguchi method in tuning the gains and orders of a FOPID controller which is designed to regulate the output force of the FUM-LSEA. A simplified model of the actuator is derived which shows that the movement of the output link of the FUM-LSEA acts as a disturbance input. Therefore, a feed-forward term is added to the controller which compensate for the disturbances caused by the motions of the output link.

The outline of this paper is as follows; Section 2 provides dynamic modeling of the FUM-LSEA. Using this model, the FOPID controller with feed-forward disturbance compensation term is designed as presented in Section 3. The Taguchi method is introduced in Section 4 and the procedure of experimentation and the experimental results are presented in Section 5. Finally, Section 6 provides the concluding discussion.

2. Modeling

A simplified structure of the FUM-LSEA is depicted in Figure 2 which shows two separate parts of the actuator connected with an elastic element. It is noteworthy that, this structure can be easily adapted for all types of prismatic SEAs. In Figure 2, F_m denotes the motor force, m_1 represents equivalent mass of the motor attached parts including inertia of the motor shaft and the ball screw as well as mass of the nut block, K_s is the spring stiffness, C_s is the damping coefficient of the spring, C_o is viscous friction coefficient between the output link and the guide shafts, x denotes displacement of the motor, x_o is displacement of the output link and F_o is the actuator's output force.

In order to design the controller, it is assumed that the coulomb and viscous frictions are negligible [24] as well

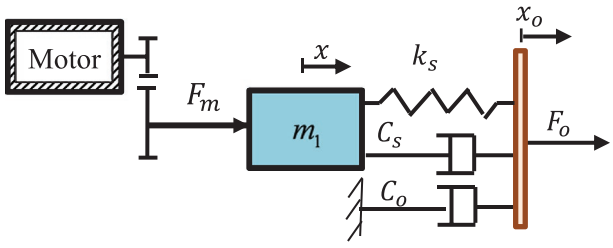

Figure 2. A simplified structure of the FUM-LSEA.

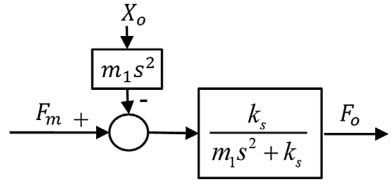

Figure 3. The block diagram of the system.

as the damping coefficient of the spring. Then, by applying Newton's law the relations between x_o, F_m and F_o can be easily obtained as,

$$m_1 \ddot{x} = F_m - k_s(x - x_o) \tag{1}$$

$$F_o = k_s(x - x_o) \tag{2}$$

By taking Laplace transform, the transfer function relating F_m and F_o can be found as,

$$\begin{aligned} F_o(s) &= \frac{k_s}{m_1 s^2 + k_s} F_m(s) - \left(\frac{k_s m_1 s^2}{m_1 s^2 + k_s}\right) X_o(s) \\ &= \frac{k_s}{m_1 s^2 + k_s}\left(F_m(s) - m_1 s^2 X_o(s)\right) \end{aligned} \tag{3}$$

Equation (3) shows how F_o is disturbed while the output load is moving. The block diagram of the SEA is shown in Figure 3.

3. Control

3.1. Fractional calculus

The operator ${}_aD_t^r f(t)$ stands for both differentiation and integration operators which are commonly used in fractional calculus. ${}_aD_t^r$ is called the fractional derivative or integral of order r with respect to variable t and with the starting point a. The operator is defined as Equation (4) [5],

$${}_aD_t^r = \begin{cases} \frac{\mathrm{d}^r}{\mathrm{d}t^r} & r > 0 \\ 1 & r = 0 \\ \int_a^t (\mathrm{d}\tau)^{-r} & r < 0 \end{cases} \tag{4}$$

Three of the most commonly used definitions for the fractional derivatives are the Grunwald–Letnikov (GL), the Riemen–Liouville (RL) and the Caputo definition [25]. The GL fractional derivative which is used in this study is expressed as Equation (5), where [.] shows the integer part.

$${}_aD_t^r f(t) = \lim_{h \to 0} \sum_{j=0}^{\left[\frac{t-a}{h}\right]} (-1)^j \binom{r}{j} f(t - jh) \tag{5}$$

For a fixed value of derivative order r, the coefficients are computed using the recursive formulas of Equations (6) and (7) [26],

$${}_aD_t^r f(t) \approx \lim_{h \to 0} h^{-r} \sum_{j=0}^{\left[\frac{t-a}{h}\right]} \omega_j^{(r)} f(t - jh) \tag{6}$$

$$\omega_0^{(r)} = 1, \omega_j^{(r)} = \left(1 - \frac{r+1}{j}\right)\omega_{j-1}^{(r)} \tag{7}$$

To design a FOPID controller and represent the time domain response of the system Laplace transform and inverse Laplace transform of non-integer order derivatives are required. The Laplace transformation is described as [25],

$$L\left[{}_aD_t^r f(t)\right] = s^r L\left[f(t)\right] \tag{8}$$

3.2. Fractional order PID (FOPID) controller

The control law of fractional order PID ($PI^{-\lambda}D^{\mu}$) controllers is defined by as,

$$u(t) = K_p e(t) + K_i D^{-\lambda} e(t) + K_d D^{\mu} e(t) \tag{9}$$

where $e(t)$ is the error signal of a tracking system, $u(t)$ is the control signal, λ and μ are positive real numbers and K_p, K_i, K_d are the proportional, integral, and derivative gains, respectively. The $PI^{-\lambda}D\hat{}\mu$ Controller is studied in time domain in [27] and in frequency domain in [28].

Control law for adjusting the output force of the actuator is proposed as given in Equation (10) and depicted in Figure 4. Note that, the feed-forward term is added to the control law to cancel out the disturbance effect, according to dynamic model of the actuator,

$$F_m = \left(K_p + K_i D^{-\lambda} + K_d D^{\mu}\right) e(t) + m_1 \ddot{x}_o \tag{10}$$

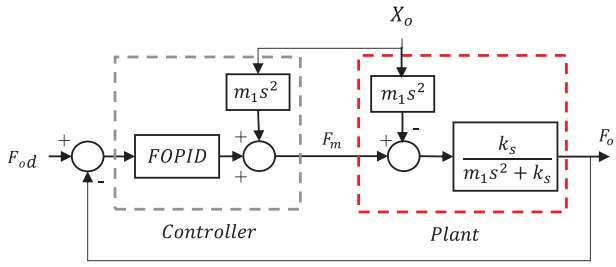

Figure 4. The proposed controller along with the SEA block diagram.

It is clear that computation of disturbance compensation term needs the second derivative of output link position which may be noise contaminated. Hence, instead of direct numerical derivative, two successive high-gain observers (HGO) are used to approximate the required velocity signals. Governing equations of HGOs are given as [29],

$$\begin{cases} x_1 = x_2 + \frac{\gamma}{\varepsilon}(y - x_1) \\ x_2 = \frac{\gamma}{\varepsilon^2}(y - x_1) \\ y = x_1 = x_o \end{cases} \tag{11}$$

in which, $y = x_1$ is the measured position signal and $\hat{x}_2$ is an estimation of the velocity signal. Also γ and ε are observer gains that determine its transient behavior and should be appropriately chosen to provide a suitable balance between noise level and delay. In this paper, the values of observer gains are set as $\gamma = 10$ and $\varepsilon = 0.005$.

4. The Taguchi method

The Taguchi method is based on the fractional factorial experiment and uses two types of parameters: design parameters for which the designer selects values as a part of the design process and noise parameters that model uncertainties in the design process.

In this paper, experimental procedure for tuning the parameters of the control law of Equation (10) is presented. The "Design of Experiment" using the Taguchi method is briefly outlined below [7]:

(1) Objectives identifications: in the first step of the Taguchi method, identifying a specific objective is important. In this paper, the objective is a robust tuning of control parameters for minimizing force tracking error.
(2) Selecting the quality characteristic: quality characteristic in the Taguchi method can be described by one of the following statements, nominal-the-best, smaller-the-better and larger-the-better. In this study, the smaller the force error, the better performance is selected.
(3) Determining the controllable factors and settings: This step is needed as the quality characteristic tests to influence the design factors, to precisely determine the design parameters, has significant importance to obtain to right conclusion. After factors selection, the desired number of levels for each factor is determined. In this paper, control parameters are selected as the controllable factors, and the number of levels for each control parameter is three. The next step is to assign a physical value to each level of controllable factors.
(4) Determining an orthogonal array: A full factorial experiment requires the testing of all combinations of the factor levels. For example, a study involving five factors at three levels each would require $3^5 = 243$ experiments. Orthogonal arrays reduce the number of required experiments. Using an $L_{27}(3^5)$ orthogonal array, for example, a study involving 5 factors at 3 levels can be conducted with only 27 experiments. In this paper, in order to reduce the number of experiments an $L_9(3^3)$ orthogonal array is selected. This array implies only nine experiments.
(5) Experiments and analysis: In this step, according to the orthogonal array which selected in previous step, the experiments must be executed. The analysis phase of experimentation relates to calculations for converting raw data into the representative Signal-to-Noise Ratio (SNR). As a measurement tool for determining robustness, the SNR is an essential component to design parameters optimally. By including the impact of noise factors on the process, the SNR can be adopted as the index of the system's ability to perform well regardless of the noise. By successfully applying this concept to experiments and analysis, it is possible to determine the control parameter settings that can produce the minimum force tracking errors while maximizing the signal to noise ratio. For this partial-fractional experiment design, the SNR in the case of smaller-the-better quality characteristic can be written as,

$$\begin{aligned} \mathrm{CF} &= W_1 \times \mathrm{NST} + W_2 \times \mathrm{MOS} + W_3 \times \mathrm{NPT} \\ \mathrm{SNR} &= -10 \log_{10} (\mathrm{CF})^2 \end{aligned} \tag{12}$$

where NST, MOS and NPT represent Normalized Settling Time (settling time divided by the total run time),

percentages of maximum overshoot, and normalized peak time (the observation time of the first peak divided by the total run time) of the SEA experimental out-put force, respectively. To normalize settling time and peak time, the corresponding values are divided by the run time that is equal to 2 s in all the experiments. W_1, W_2, and W_3 are weight coefficients and are used to make the contribution portion of each term in building the CF as the same as the other two terms. Weight coefficients are selected once at the beginning of the experiments and are kept fix within all the experiments and the simulations. Here, W_1 and W_2 are selected the same and equal to 10 and W_3 is selected as 100. The defined performance criteria, CF, are simply computable, and provide fast closed loop responses with low overshoots.

Since the Taguchi method reduces the number of experiments over the full-factorial approach, the statistical analysis of experiments, called analysis of variance (ANOVA), should be applied to evaluate levels of confidence in the results. Moreover, analysis of variance identifies and ranks variables that affect the variance of the output signal. The ANOVA is one of the main steps in using the Taguchi method.

5. Experiments

A Test setup is prepared for implementation of the designed control algorithm. As shown in Figure 5, the test setup is a linear stage actuated by a 200 W AC servo motor and a ball screw mechanism. The test setup is designed such that the SEA is easily placed on the top and its output link is fixed to the moving block of the linear stage as shown in Figure 6.

When the position of the servo motor of the test setup is locked, the moving block, and consequently the output link of the FUM-LSEA, cannot displace. The mentioned mode is of the interest when it is desired to have the actuator to apply some force trajectories in fixed lengths. If the position of the servo motor of the test setup is changed, the moving block and the output link of the FUM-LSEA start

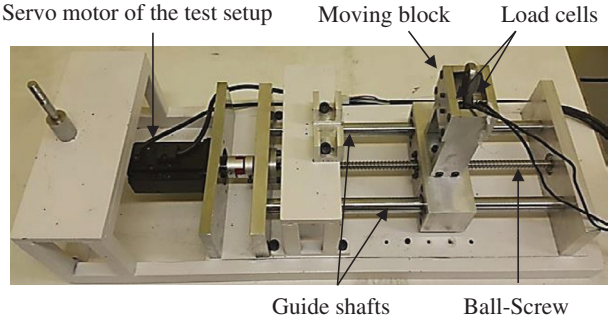

Figure 5. The linear stage test bed for evaluation of the control algorithm.

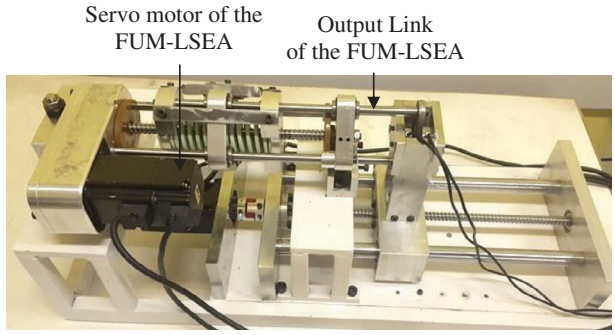

Figure 6. FUM-LSEA placed on the linear stage test bed.

to move. This mode is of the interest when it is desired to have the actuator to apply some force trajectories while the output link is moving arbitrarily. Actually, the servo motor of the test setup is used to apply arbitrary motions to the output link of the FUM-LSEA.

Two load cells are placed at the connection point of the actuator and the linear stage test bed. These load cells are merely used for monitoring purposes and obviously do not contribute in implementation of the control algorithm.

Actually, the test bed is designed to evaluate the performance of different force controllers designed for the FUM-LSEA, in the presence of some disturbances resulted from arbitrary motions of the output link. A good force controller should be able to perfectly apply the desired output force trajectories despite the arbitrary motions of the output link.

5.1. Performance evaluation of the test bed

A test is designed to evaluate the performance of the setup which is important to guarantee the precise motion of the output link. Figure 7(a) shows the desired and actual motion of the output, while the error signal is shown in Figure 7(b). As illustrated in Figure 7(b), the error signal is less than ±1 mm which is negligible.

As explained before, two different tests can be performed to assess the performance of the designed controller. In the first test, the moving block of the linear stage test bed is locked which consequently results in locking the output link of the actuator, i.e. $X_o = 0$. The output force is then controlled to follow the desired trajectory. In the second test, the FUM-LSEA is controlled to exert desired output forces while the moving block of the test bed and consequently the output link of the SEA are displaced in an arbitrary path.

Clearly, the experiment with the moving output link provides a better evaluation of the force controller. This is true because when the output link of the FUM-LSEA is moving, the force controller should track the desired output force trajectories while compensating the disturbances

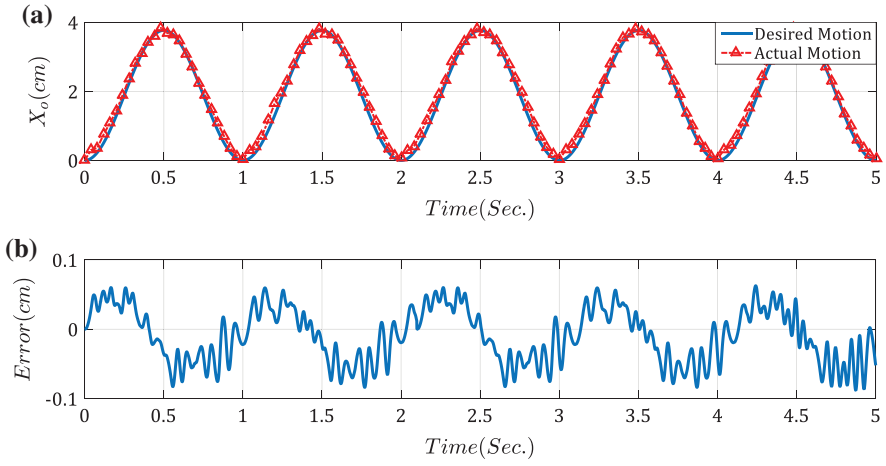

Figure 7. Evaluation of the setup accuracy; (a): Desired vs. actual motion of the setup, (b): Position error.

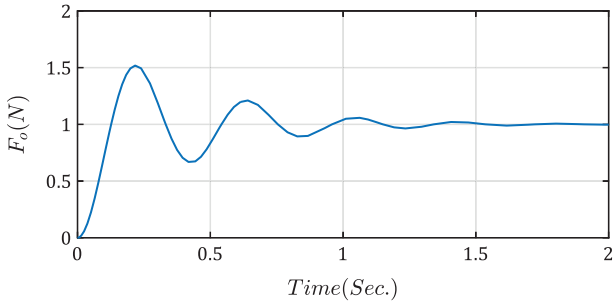

Figure 8. Time response of the closed loop system with Z–N-tuned FOPID controller.

Table 1. System parameters.

Parameter	k_s (N/m)	m_1 (kg)
Value	60	0.7

Table 2. The initial values for FOPID controller obtained from Z–N method.

Parameter	K_p	K_i	λ	K_d	μ
Value	0.6	0	–	3.0	0.3

resulted from the motions of the output link. Therefore, the tuning experiments are performed while the output link is moving. However, after the Taguchi- and Z–N-tuned controllers are obtained, the performances of the controllers are evaluated and compared in both experiments with clamped and moving output link.

5.2. Initializing

The value of the parameters of the dynamic model which is presented in Section 2 are listed in Table 1.

Table 3. Experimental layout based on $L_9(3^3)$.

# of runs	1	2	3	4	5	6	7	8	9
K_p	1	1	1	2	2	2	3	3	3
K_d	1	2	3	1	2	3	1	2	3
μ	1	2	3	2	3	1	3	1	2

Table 4. Levels of the parameters.

Parameter	1st level	2nd level	3rd level
K_p	0.5	1	5
K_d	0.3	3	9
μ	0.3	0.6	1.3

Table 5. Orthogonal array for FOPD controller with corresponding outputs.

# of runs	K_p	K_d	μ	CF	SNR
1	1	1	1	28.13	−43.11
2	1	2	2	27.52	−42.02
3	1	3	3	22.72	−32.89
4	2	1	2	18.25	−25.80
5	2	2	3	21.45	−31.95
6	2	3	1	17.96	−25.39
7	3	1	3	20.15	−27.12
8	3	2	1	19.58	−26.31
9	**3**	**3**	**2**	**17.82**	**−24.91**

The initial values for the experimentation are provided in Table 2. These values are found by applying the Ziegler–Nichols (Z–N) technique to the theoretical model of the FUM-LSEA [30]. As shown in Figure 8, time response of the Z–N-tuned closed-loop system to a unit step input contains a relatively high overshoot as well as sustained oscillations. The CF value for this simulation is obtained as 19.92. Note that Figure 8 is obtained through simulating the theoretical model of the FUM-LSEA with a unit step desired output force while the output link of the actuator is clamped.

The fact that the gain tuning by Z–N gives the value of zero for the integrator gain of the controller, indicates

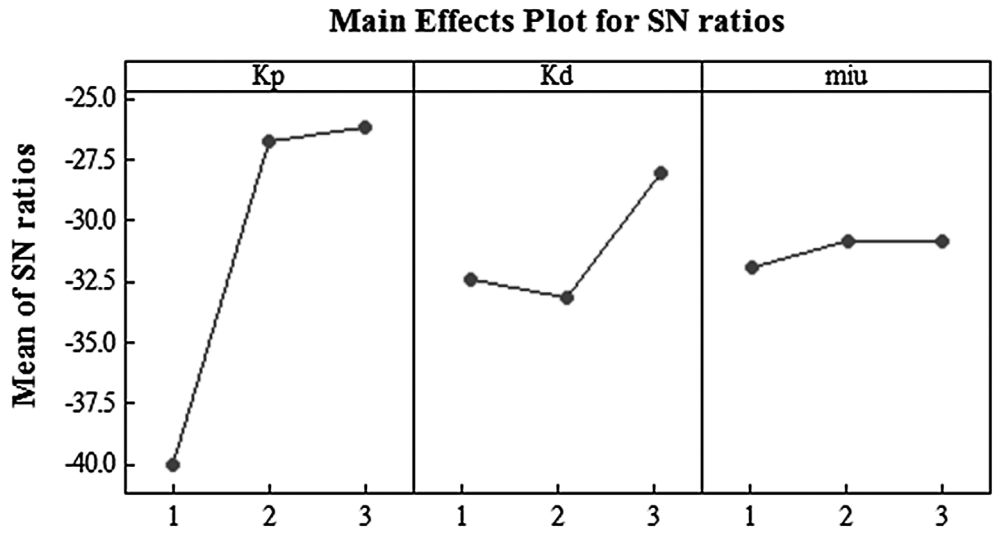

Figure 9. Main effects plot for SN ratios.

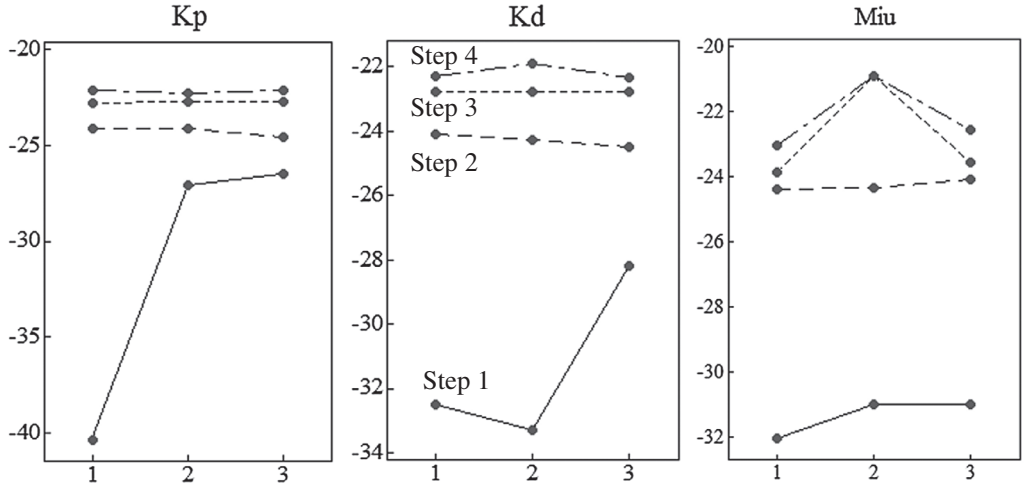

Figure 10. Main effects plots for SN ratios for the four steps of optimization.

Table 6. Levels of control parameters in steps 2 to 4.

	Step 2			Step 3			Step 4		
Parameter	1st level	2nd level	3rd level	1st level	2nd level	3rd level	1st level	2nd level	3rd level
K_p	4	5	8	4.9	5	5.2	4.7	4.9	5.0
K_d	8	9	12	8.9	9	9.2	8.9	9	9.1
μ	0.5	0.6	0.7	0.7	0.9	1.1	0.8	0.9	1.0

Table 7. CF and SNR values for the steps 2 to 4.

	Levels			Step 2		Step 3		Step 4	
# of run	K_p	K_d	μ	CF	SNR	CF	SNR	CF	SNR
1	1	1	1	16.14	−24.16	15.84	−23.99	14.18	−23.03
2	1	2	2	15.91	−24.03	**11.00**	**−20.82**	**11.01**	**−20.83**
3	1	3	3	16.01	−24.09	15.03	−23.53	14.16	−23.02
4	2	1	2	16.03	−24.10	11.13	−20.93	11.13	−20.93
5	2	2	3	**15.84**	**−23.99**	15.12	−23.59	13.05	−22.31
6	2	3	1	17.13	−24.67	15.43	−23.77	13.15	−22.38
7	3	1	3	16.24	−24.21	15.10	−23.58	13.13	−22.36
8	3	2	1	16.34	−24.26	15.46	−23.78	15.29	−23.69
9	3	3	2	17.67	−24.94	11.20	−20.98	11.20	−20.98

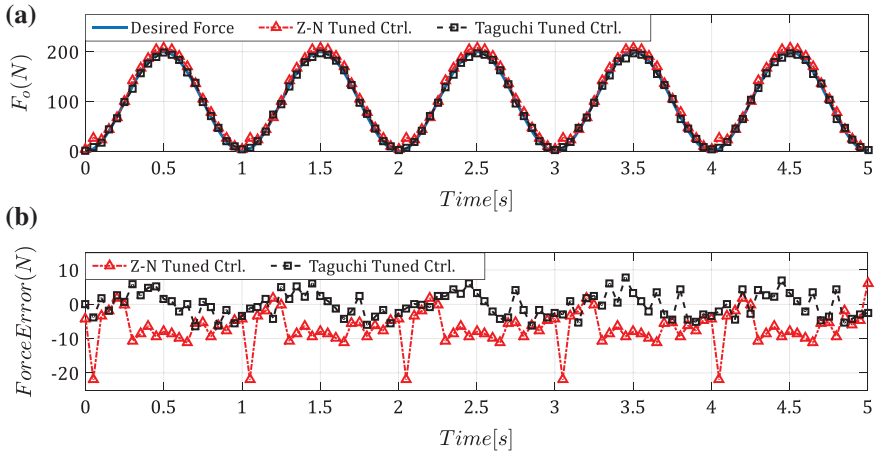

Figure 11. Force tracking performance of the closed loop system with clamped output block.

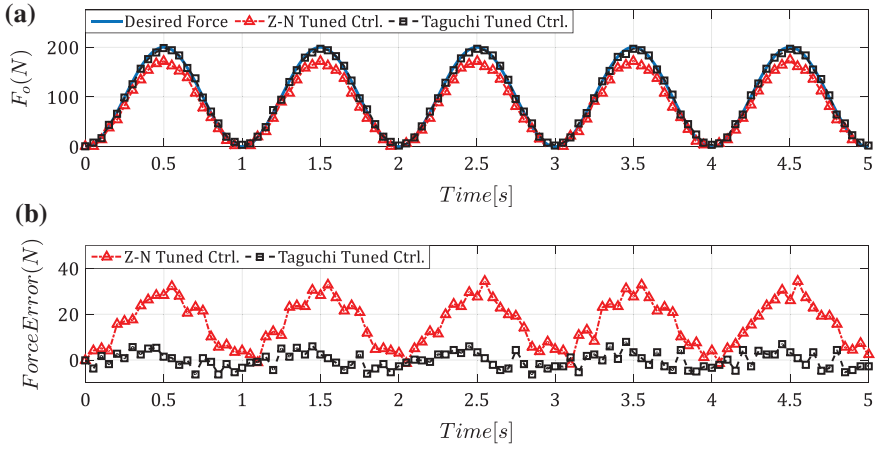

Figure 12. Force tracking performance of the closed loop system with moving output block.

Table 8. Percentage contribution.

Control parameter	Percentage contribution (%)	*P*-value
K_p	5.40	0.62
K_d	5.97	0.59
μ	79.81	0.09
ANOVA error	8.81	

that the integrator term has no effect on the system performance. Therefore, during the experimental gain tuning procedure, only tuning of the coefficients and order of the differentiator and proportional terms will be considered. It is worth to mention that at this situation, the FOPD controller with only three degrees of freedom is still more flexible than the regular PID controllers. The reason is that having the option of choosing the fractional order of the differentiator makes the controller non-linear which can better deal with practical systems.

5.3. The Taguchi table and results

From Table 2 it is found that the initial value for fractional order integrator gain is obtained equal to zero, this corresponds to FOPD controller, then the number of parameters in FOPID controller reduces to three parameters. Again there is a need to determine the appropriate orthogonal array. A $L_9\left(3^3\right)$ is determined in this step. The experimental layout is shown in Table 3. The nine columns of this matrix represent the experiments to be conducted. The three rows correspond to three parameters or factors. Levels of the parameters are shown in the Table 4.

The experiments were carried out for each level and the errors were calculated for each experiment. Then the experimental values of CF and SNR were calculated for each test. The SNR values were calculated based on smaller the better characteristics. The sum of SNR was calculated for each parameter and at each level as shown in Table 5. Figure 9 shows the graphs of the average response value for each factor level. These graphs reveal the relative effect of each parameter on the performance criterion.

The Mean effect plots are obtained using the Minitab Statistical Software which reports the average of the SNR values for each level of the corresponding factor. For example, the parameter K_d is in its first level in the 1st, 4th, and 7th rows of Table 5. The average of SNR values in the

these rows of Table 5 is about –32.5 which is also depicted in Figure 9 as the mean of SNR for the first level of K_d.

The response graph indicates that factor K_d has the strongest effect on the SNR, whereas K_p and μ have weak effects. Based on Table 5, the optimum level of each parameter i.e. the levels that result in a maximum SNR are those in experiment number 9. From the 1st step of tuning of controller's parameters with Taguchi method, the error is reduced by 10%.

Considering Figure 9, it is observed that the preferred levels for K_p, K_d, and μ are set at 3rd, 3rd, and 2nd levels, respectively. The SNR value for K_p and K_d increases for successive levels. This means that values for K_p and K_d that can maximize the SNR may be larger than the chosen levels. Therefore, the levels of theses parameters in the next step should be chosen above their 3rd level values in the first step. However, in the case of the parameter μ, the levels in the next step should be refined around the value of the 2nd level in the first step. Accordingly, based on the levels in the step 1, control parameters should be further tuned in step 2.

In the second step, the experimental procedure is the similar to the gain tuning of the step 1 except for the levels of control parameters. After conducting gain tuning in the step 2, if it is possible to increase the SNR, additional gain tuning steps should be performed. Following this instruction, the Taguchi gain tuning process is completed in four steps. Table 6 represents the levels of control parameters selected in the steps 2 to 4. The CF and SNR values for these steps are provided in Table 7 and the preferred levels for control parameters in each step are indicated by bold font.

As depicted in Figure 10, response graphs of the step 4 show that the SNR for K_p, K_d and μ do not increase any further and the preferred levels are the first level for K_p and the second level for K_d and μ. This means that their optimal levels exist around these values and the control parameters are finally tuned in the step 4.

Force tracking performances of the two controllers (FOPID controller tuned by Z–N technique and final FOPID controller tuned by Taguchi method) are shown in Figures 11 and 12. In the experiment of Figure 11 the output link of the FUM-LSEA is clamped ($X_o = 0$) while in the experiment of Figure 12, X_o is moved in the same path of the Figure 7.

Considering Figures 11 and 12, it can be observed that the FOPID tuned by Taguchi method provides better tracking performance, compared to the Z–N-tuned FOPID controller. Comparison of the closed loop systems performance shows a 45% improvement in actuator's force tracking error for the system with moving output block and 55% improvements in the same performance criteria for the system with clamped output block.

Results are confirmed by the ANOVA analysis with the percentage contribution shown in Table 8. The main purpose of this analysis is to estimate the effects that each factor has on the final results. ANOVA analysis shows that μ parameter has the biggest percentage contribution. It confirms results of Figure 10 which illustrates that SNR values for the levels of μ differ significantly in the step 4. It is important to note that the error contribution computed with ANOVA gives an idea of the confidence in the results. *P*-values which are shown in second column also confirm that the variations of parameters K_p and K_d in the step 4 do not have important effects on improvement of SNR value.

6. Conclusion

In this paper, an experimental verification of a recently proposed gain tuning method is carried out. The controller also is enhanced by adding a feed-forward term for disturbance compensation. The proposed gain tuning method is based on the Taguchi statistical technique of the design of experiments and is used to adjust the output force of a SEA using a FOPID controller. To determine the initial range of values for the control parameters, a Ziegler–Nichols tuning method was used. Control parameters were next tuned through four optimization steps. In each step, a balanced orthogonal array $L_9(3^3)$ was used to design the experiment. Results of each step were used to determine the proper settings for the next step. The CF performance criterion was selected to make the closed loop response to have low overshoots and fast responses. A custom-made prismatic SEA was developed and constructed to perform the experiments. Additionally, a linear stage equipped with a position encoder and load cell feedbacks is constructed. Two sets of experiments with clamped and moving SEA's output block were used to evaluate the force tracking performance of the closed loop system. Since the experiment with the moving output link provides a better evaluation of the force controller, the optimization process was carried while the output link of the actuator was moving. Comparison of the results of the proposed method with results obtained from the regular FOPID controller illustrated that FOPID tuned by Taguchi method gives better time domain performance. Specifically, comparison shows a 45% improvement in actuator's force tracking error. The same optimized settings were then used for some clamped block experiments. Results also showed a 55% improvement in actuator's force tracking error. Finally, ANOVA results showed the contribution percentages of 5, 6, and 78% for the controller parameters, parameters K_p and K_d and μ, respectively. *P*-values also confirm that variation of the derivative and the proportional gains have no significant effects on improvement of the SNR value.

Acknowledgements

This study was financially supported by Ferdowsi University of Mashhad (Grant No 21786).

Disclosure statement

No potential conflict of interest was reported by the authors.

Notes on contributors

Somayeh Norouzi Ghazbi received her MSc degree in Mechanical Engineering from Ferdowsi University of Mashhad (FUM) in 2013. Her MSc project was on control and modeling of aerial vehicles. From 2013, she started her research at Robotic Lab of FUM on Biomedical robots, exoskeletons. Her research interests include control, image processing, machine learning, and mathematical modeling.

Alireza Akbarzadeh received his PhD in Mechanical Engineering in 1997 from the University of New Mexico in USA. He worked at Motorola, USA, for 15 years where he led R&D as well as automation teams. He joined the Ferdowsi University of Mashhad in 2005 and is currently a full professor in the Mechanical Engineering Department. His areas of research include robotics (parallel robots, biologically inspired robots, bipedal robots and rehabilitation robotics), dynamics, kinematics, control, automation, optimization as well as design and analysis of experiments. He is also a founding member of the Center of Excellence on Soft Computing and Intelligent Information Processing (SCIIP).

Iman Kardan received his PhD in Mechanical Engineering from Ferdowsi University of Mashhad, Mashhad, Iran in 2017. He is currently a research assistant at robotic laboratory of Ferdowsi University of Mashhad. His research interest is in the areas of robotics (parallel robots, serial manipulators, rehabilitation robots and exoskeletons), control, microrobotics and smart materials.

ORCID

Alireza Akbarzadeh http://orcid.org/0000-0001-8605-8956
Iman Kardan http://orcid.org/0000-0002-5520-1577

References

[1] Accoto A, Carpino G, Sergi F, et al. Design and characterization of a novel high power series elastic actuator for a lower limb robotic orthosis. Int J Adv Rob Syst. 2013.
[2] Pratt G, Williamson M. Series elastic actuators. In: Proceedings of IEEE/RSJ International Conference on Intelligent Robots and Systems; Pittsburgh, PA; vol. 1; 1995. p. 399 –706.
[3] Pratt J, Krupp B, Morse C. Series elastic actuators for high fidelity force control. Ind Robot Int J. 2002;29(3):234–241.
[4] Kamali K, Akbari A, Akbarzadeh A. Trajectory generation and control of a knee exoskeleton based on dynamic movement primitives for sit-to-stand assistance. Adv Rob. Forthcoming.
[5] Au SK, Dilworth P, Herr H. An ankle-foot emulation system for the study of human walking biomechanics. International Conference on Robotics and Automation; Orlando, FL; 2006 May.
[6] Kong K, Bae J, Tomizuka M. Control of rotary series elastic actuator for ideal force-mode actuation in human-robot interaction applications. IEEE/ASME Trans Mechatron. 2009;14(1).
[7] Taylor DM. A compact series elastic actuator for Bipedals with human-like dynamic performance [MSc thesis]. Carnegie Mellon University; 2011.
[8] Hutter M, Remy CD, Hoepflinger MA, et al, High compliant series elastic actuation for the robotic leg scarIETH. International Conference on Climbing and Walking Robots (CLAWAR); Paris; 2011 Sep 7.
[9] Misgeld BJE, Gerlach-Hahn K, Rüschen D, et al. Control of adjustable compliant actuators. Machines 2014;2(2):134–157.
[10] Wang M, Sun L, Yin W, et al. A novel sliding mode control for series elastic actuator torque tracking with an extended disturbance observer. In: 2015 IEEE International Conference on Robotics and Biomimetics (ROBIO); Zhuhai; 2015. p. 2407–2412. DOI:10.1109/ROBIO.2015.7419699
[11] Kaya KD, Levent Ç. Adaptive state feedback controller design for a rotary series elastic actuator. Trans Inst Meas Control. 2015.
[12] Podlubny I, Dorcak L, Kostial I. On fractional derivatives, fractional-order dynamic systems and PID controllers. IEEE Transactions on Automatic Control; San Diego, CA; 1997.
[13] Vinagre BM, Podlubny I, Dorcak L, et al. On fractional PID controllers: a frequency domain approach. In: Proceedings of IFAC Workshop on Digital Control: Past, Present and Future of PID Control; Terrasa, Spain; 2000. p. 53–58.
[14] Monje CA, Vinagre BM, Chen YQ, et al. Proposals for fractional *PIλDu* tuning. Proceedings of Fractional Differentiation and its Applications; Bordeaux; 2004.
[15] Valério D, da Costa JS. Tuning of fractional PID controllers with Ziegler–Nichols-type rules. Signal Process. 2006;86:2771–2784.
[16] Zamani M, Karimi GM, Sadati N, et al. Design of a fractional order PID controller for an AVR using particle swarm optimization. Control Eng Practice. 2009;17(12).
[17] Monje A, Blas M, Vinagre M, et al. Tuning and auto-tuning of fractional order controllers for industry applications. Control Eng practice. 2008;16(7).
[18] Lee K, Kim J. Controller gain tuning of a simultaneous multi-axis PID control system using the Taguchi method. Control Eng practice. 2000;8(8).
[19] Ryckebusch EF, Craig IK. PID tuning for a multivariable plant using Taguchi-based methods. Proceedings of the 15th IFAC World Congress; Barcelona, Spain; 2002.
[20] Alfaro VM, Vilanova R, Arrieta O. Maximum sensitivity based robust tuning for two-degree-of-freedom proportional–integral controllers. Ind Eng Chem Res. 2008.
[21] Santhakumar M, Asokan T. A self-tuning proportional-integral-derivative controller for an autonomous underwater vehicle, based on Taguchi method. J Comput Sci. 2010;6(8):862–871.
[22] Ghazbi SN, Akbarzadeh A. Prismatic series of elastic actuator: modelling and control by ICA and PSO-tuned fractional order PID. Int J Adv Des Manuf Technol. 2016;8(4).

[23] Ghazbi SN, Akbarzadeh A. Fractional order PID Design using the Taguchi method. IAES Int J Rob Autom (IJRA) 2015;4(3).
[24] Williamson MM Series elastic actuator [MSc thesis]. Massachusetts Institute of Technology Artificial Intelligence Laboratory; 1995.
[25] Vinagre BM, Podlubny I, Petras I, et al. Using fractional order adjustment rules and fractional order reference models in Model Reference Adaptive Control. Nonlinear Dyn. 2001;29:269–279.
[26] Monje CA, Chen YQ, Vinagre BM. Fractional order systems and controls fundamentals and applications. Springer Science & Business Media; 2010.
[27] Podlubny I. Fractional-order systems and *PIλDu* controllers. IEEE Trans Autom Control. 1999;44(1):208–214.
[28] Petr′aˇs I. The fractional-order controllers: methods for their synthesis and application. J Electr Eng. 1999;50(9–10):284–288.
[29] Vasiljevic LK, Khalil HK. Differentiation with high-gain observers the presence of measurement noise. In" IEEE Conference on Decision and Control; 2006 December 13–15; San Diego, CA; p. 4717–4722.
[30] Valério D, da Costa JS. Tuning of fractional PID controllers with Ziegler–Nichols-type rules. Signal Process. 2006;86(10):2771–2784.